Journal Homepage: -www.journalijar.com

INTERNATIONAL JOURNAL OF ADVANCED RESEARCH (IJAR)

Article DOI:10.21474/IJAR01/17451
DOI URL: http://dx.doi.org/10.21474/IJAR01/17451

RESEARCH ARTICLE

Variable hydropyrolysisreactivity of kerogen from Tarfaya oil shale deposit (Morocco). Modeling in heterogeneous kinetics

Abdeljabbar Attaoui
DepartmentofChemistry,FacultyofSciencesBenm'sikCasablanca, UniversityHassanIIMorocco.

Manuscript Info

Manuscript History
Received: 25 June 2023
Final Accepted: 29 July 2023
Published: August 2023

Abstract

Hydrogen treatment of oil shale kerogen is highly beneficial, firstly because it improves the yield of oil produced compared with pyrolysis, secondly because the oils produced are of light quality and thirdly because the kinetics of this heterogeneous reaction are simpler **(A.Attaoui: 2023).** The latter, often discussed in true thermogravimetry (dynamic regime), can be adapted to several mathematical models for processing values.In this work we are going to follow this primary hydropyrolysis reaction in the dynamic regime using thermogravimetry, and we are going to develop a method for processing the experimental values in order to access the energies of the different oil shale layers at different heating rates.The aim of this study is to establish the activation energy balance for the different layers of the Tafaya primary hydropyrolysis deposit. We used the Red-Croft thermobalance to carry out these reactions. We note the close dependence between the experimental technique, the data processing model and the activation energies search for.

Introduction:-

The method of analysis and mathematical modeling of the thermal decomposition of oil shale make it possible to achieve kinetic parameters. For the hydropyrolysis reaction we note that the effects of hydrogen on oil shale differ according to their variety. MinoraEnomoto et al **(M. Enomoto et al: 1985)** carried out a series of experiments on shale from Colorado and Thailand, to study the effects of the different operations on the yield and performance of the process at high hydrogen pressures. The lightest oils are obtained from oil shale, whose yield is insensitive to hydrogen pressure. However, by increasing the gas flow rate, the yield increases slightly, so the oil becomes heavy, especially in the case of oil shale from Colorado. The effect of gas pressure and flow rate (H_2) is more complex. The maximum capacity for this process is determined for shale with an apparent thermal conductivity estimated at 0.04 kcal/m.h.°C. In addition, using a hydrogen balance **(M. Enomoto et al: 1982)**, these authors found that significant amounts of hydrogen are consumed during the degradation of shale, and that this consumption increases as the pressure increases. Similarly, it was found that the type of reactor slightly affects the properties of the oils. It probably appears that a remarkable quantity of sulphides in raw shale remains trapped during decomposition by calcium varieties which are retained in the ash **(E. Fuzimsky at al: 1984).** It has also been noted that the presence of hydrogen reduces the density of the oil produced and the concentration of sulphides, but increases the concentration of nitrogen. This increase is attributed to the stability of nitrogen compounds in the presence of hydrogen.

Corresponding Author:- Abdeljabbar Attaoui
Address**:-**
DepartmentofChemistry,FacultyofSciencesBenm'sikCasablanca,UniversityHassanIIMorocco.

1/ Literature Review:-

The Hytort process **(P.A. Lunch and J.C. Janta et al: 1984)** was developed by several American organizations. This process operates under hydrogen pressure, the effect of which on the shale differs according to their variety **(S.D. Carter et al: 1990);** similarly, it has been found that a remarkable quantity of sulphides in raw shale remains trapped during decomposition by calcium varieties and passes into the ash. For example, the Green River shale in the western United States contains a high concentration of hydrogen relative to organic carbon, and yields a high yield simply by decomposition using the conventional procedure and an inert gas. In contrast, many other shale similar to the Devonian in the eastern United States contain a lower concentration of hydrogen than Green River **(J.C. Janka, R.C. Rex: 1984)**, and this hydrogen deficiency prevents much of the kerogen from being converted to hydrocarbons **(J.C. Janka and J.M. Dennison: 1979, R.D. Matews et al: 1981)**. The yield obtained from the conventional decomposition of this shale can be improved by adding more hydrogen during the degradation process, which allows more of the kerogen to be converted into hydrocarbons rather than remaining in the ash in the form of coke.

The equilibrium and kinetic data will be described by two reversible oxidation and reduction reactions. These two reactions allow the transformation mechanism to be managed qualitatively, the rate to be measured and expressed. In addition, the hydrogenation of CO can give methane by catalytic reaction [Bimetallic Mo-Fe. and sulphureted Mo-Co fixed on alumina]. By adding methane, a significant quantity of dimethyl ether was produced.

Thermogravimetry and its derivatives (TG / DTG) have been used to evaluate the kinetics of the studied oil shale. Based on the complexity of the pyrolysis mechanism, a multi-peak fitting method was applied to separate the overlapping processes using the asymmetric Fraser-Suzuki function. For each separated process, the activation energies were determined by the Kissinger-Akahira-Sunose (KAS) and Flynn-Wall-Ozawa (FWO) integral methods and the Friedman differential isoconversion (FR) method. The Coats-Redfern fitting method was used to ensure the activation energy and thus to confirm the proposed kinetic model. Thermogravimetric analysis was used to quantify the mass change of a sample as a function of temperature and time, under controlled atmosphere, simultaneous TG / DTG / DTA analyses were performed on a LabsysTMEvo (1F) Setaram instrument. The ICTAC Kinetics Committee recommendations for collecting experimental data and performing kinetic calculations were followed to evaluate the kinetic parameters **(Vyazovkin S et al; 2011)**. Prior to analysis, the thermal analysis system was calibrated for temperature readings with reference metals of 99.99% purity.

In the non-isothermal regime, several mathematical models have been put forward by authors **(A.W.CoastandD.P.Redfern: 1964, Z.S. Freeman and B. Carroll: 1952, D.B. Anthony and J.B. Howard: 1976, H.L.Friedman: 1965, S.M. Shin and H.Y. Sohn; 1980, M. Suziki et al: 1980)** as well as the extension of Arrhenius'law, for the evaluation of kinetic parameters. Let us recall that all these models have the Arrhenius law as theirmathematical basis and according to the approximate form of its resolution, we obtain the different laws mentionedandwhichareattributedtotheirauthors.Theauthors**(LeeandBeck:1984)**madesomedevelopments andapproximations bytheintegralmethodandwhichwereproposedearlierbytheauthors**(V.M.Gorbachev:1976, R.K. Agrawal, et al: 1987)** made in the same vision by their approximations, the authors **(S.V. Vyazovkin et al:1987)** made a method of approach, they noted that the nontraditional method gives great information that thetraditional one. Authors **(J.E. Cuthrell et al: 1987)** optimized differential systems into algebraic systems by amethod based on finite collocation elements to algebraic equations in the residual nonlinear model knowing thefactorialandadditivecoefficients.Similarlytheauthors**(Z.Smieszekietal:1988)**usedmethodsforthedeterminationofki netic constantsandnotedthe significant effect ofthemethod onthe estimatesofthe results.

2/ Experimental techniques

2.1: Thermogravimetry

The thermal analysis technique of thermogravimetry (TG) is one in which the change in mass of the sample (loss of mass or grain) is determined as a function of temperature and/or time. Three modes of thermogravimetry are commonly used, isothermal thermogravimetry in which the mass of the sample is recorded as a function of time at a constant temperature; quasi-isothermal thermogravimetry, in which the sample is heated to a constant mass at each of a series of increasing temperatures; and dynamic thermogravimetry in which the sample is heated in an environment whose temperature undergoes a change in a predetermined way, preferably at a linear rate. Most of the studies reviewed will refer to dynamic thermogravimetry, which is referred to as the resulting mass change versus temperature curve (which has various synonyms such as thermoanalysis curve, pyrolysis curve, thermograms, thermogravimetric curve, thermogravimetric analysis curve, etc.) it gives information regarding the thermal stability

and composition of the starting sample. The thermal stability and composition of all the intermediate compounds that can be formed, and the composition of the residue, this being to provide useful information with this technique.

The sample must evolve to a volatile product, which can come from various physical and chemical processes. Much of the information obtained from the TG curve is empirical in nature and that the transition temperatures depend on the instrumental parameters and the sample. The following picture shows a thermobalance from the Setaram series called Red-Croft, which is a flail thermobalance with a compensation system based on a photoelectric source to keep the sample at the same position in the oven, avoiding the temperature gradient due to a displacement of the sample in the oven.

Figure1:- Photo ofthermobalance Red-Crof.

2.2: Thermogravimetric results.

The following experiments were carried out in a dynamic thermal regime at three heating rates of 9, 15 and 21°C/min up to 750°C in a hydrogen atmosphere (PH_2 = 1atm, flow rate = 20 cm^3/min) on samples with a particle size of 0.25 mm and a mass of approximately 15 mg. The thermograms obtained for samples from zones 0, 1, 2, 3 and 4 of the Tarfaya deposit are shown in figures 3, 4 and 5, expressed in Δm/mo = f(T) for each heating rate. Figure 6 also shows the degradation under hydrogen for samples Z2 and Z3, expressed as

Δm /mo = f (T) at each heating rate. In all the figures we observe three distinct regions of mass loss, as in the case of pyrolysis:

*a first slight loss related to the departure of water and volatile gases,

***a second loss relating to the degradation of organic matter (a stage known as primary hydropyrolysis)**

*and then a third loss relating to the decomposition of carbonates.

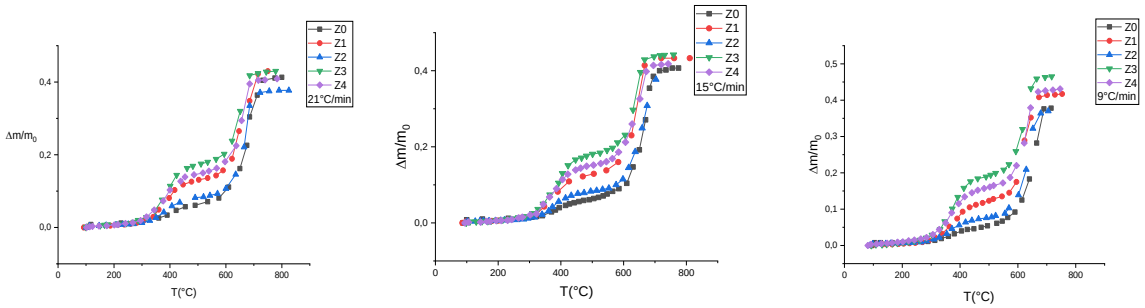

Fig 2:-Decomposition of oil shale in $\Delta m/m_0$=f (T) into hydrogen carrier gas of the different layer ofTarfaya at different heating rates (Θ=21°C/min, Θ=15°C/min and Θ=9°C/min)

The following table shows the percentages of mass loss during hydrogen degradation of organic matter and the temperatures of the DTG peaks for each sample and for the three heating rates indicated.

Table 1:- Percentage loss (MO) and DTG peak temperatures for thehydrotraitement reaction.

Heating rate (°C/min)	**Characteristics**	**samples**				
	Origin	Tarfaya				
	Zone	Z_0	Z_1	Z_2	Z_3	Z_4
21	Percentage loss	6,5	12,3	7,4	16,4	14,4
	DTG peak temperature	-	427	404	401	398
15	Percentage loss	5,6	11,6	7,7	18,09	15,59
	DTG peak temperature	-	411	386	390	377
09	Percentage loss	5,0	11,59	6,89	18,4	15,1
	DTG peak temperature	-	392	373	379	368

Based on these results, we can see that the layers contain varying quantities of hydrocarbons, which we classify in descending order: Z3, Z4, Z1, Z2 and Z0. The Z3 layer is far superior to the others. The thermograms of the different layers, expressed in □ =f (T) fig (3, 4 and 5) at different heating rates, show the same curves except for Z0; their reactivity is therefore similar.

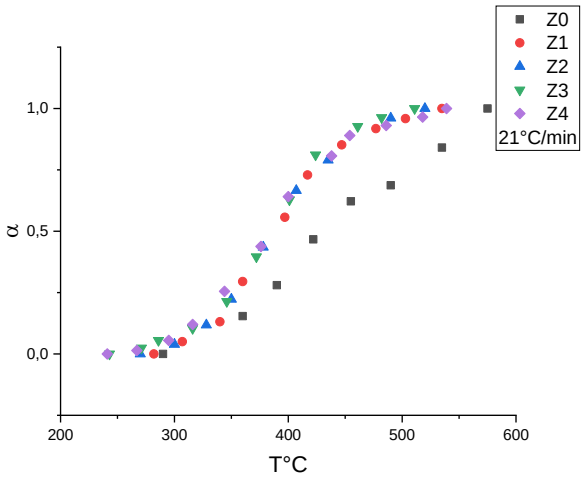

Fig 3:- Thermograms in α of the hydropyrolysis of the different Tarfaya layers at Θ=21°C/min.

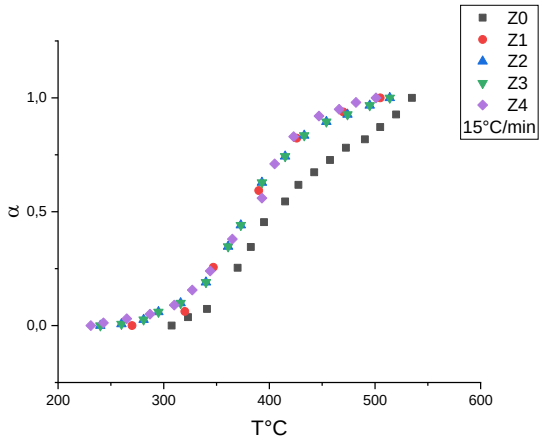

Fig 4:- Thermograms in α of the hydropyrolysis of the different Tarfaya layers at Θ=15°C/min.

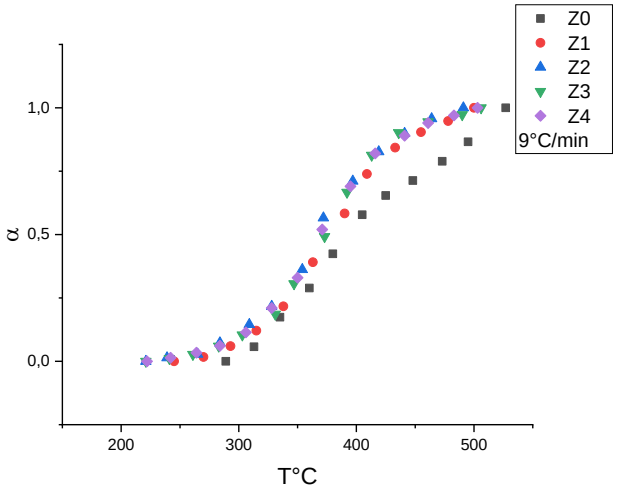

Fig 5:- Thermograms in α of the hydropyrolysis of the different Tarfaya layers at Θ=09°C/min.

To observe the effect of the heating rate on the decomposition reaction, Figures 6 and 7 show the αhydropyrolysis of successive layers Z2 and Z3.

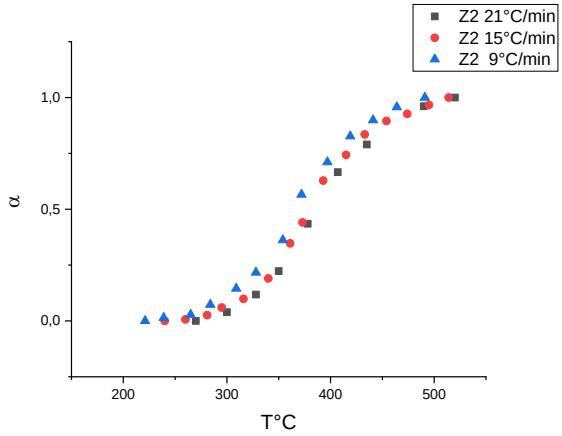

Fig 6:-Thermograms in α of the hydropyrolysis of the Z2 layer at the three heating rates.

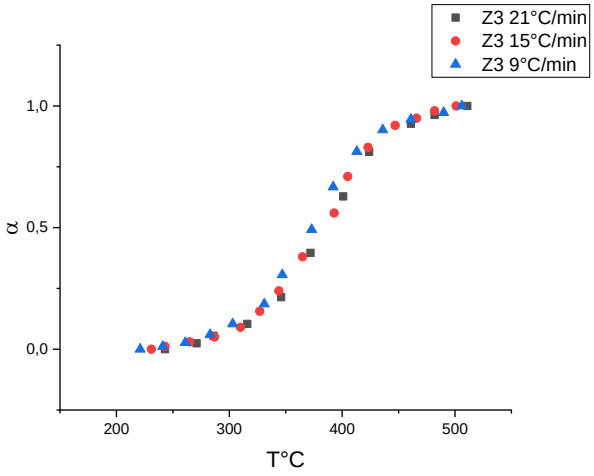

Fig 7:-Thermograms in α of the hydropyrolysis of the Z3 layer at the three heating rates.

A slight offset is felt due to the heating rate.
The position of the curves α=f(T) in relation to each other indicates that the samples have similar reactivity, whereas for the DTG, a difference in the maximum temperature of the peaks can be noted, which we will try to discern later. This shows the reactive effect of hydrogen on the same type of organic matter, where the determining stage is the same.

Shale samples with different relativity an inert gas will have the same reactivity in the presence of hydrogen.

The kinetic order of this reaction has been studied **(A.Attaoui: 2023)** and is equal to unity. In addition, the organic matter concentration threshold, above which hydropylosis is the same for all the samples, is 6.86% apart from Z0. The low reactivity of Z0 compared to the other zones can be explained by its low organic matter concentration. It has been shown that pyrolytic oil acts as a catalyst during thermal degradation **(K.M. Jeong and J.F. Patzer: 1983).**

2.3: Analysis of thermograms for Z2 and Z3 in terms of degree of advancement α (Θ=21°C/min)
The following two tables show the degree of advancement α of primary hydropyrolysis (decomposition of organic matter (kerogen) under hydrogen) as a function of temperature

Z2

α	T°C
0	270
0,04	300
0,12	328
0,22	350
0,44	378
0,67	407
0,79	435
0,96	490
1	520

Z3

α	T°C
0	243
0,06	286
0,10	316
0,21	346
0,40	372
0,63	401
0,81	424
0,93	461
1	511

The following curve represents these thermograms of hydropyrolysis in α= f(T)

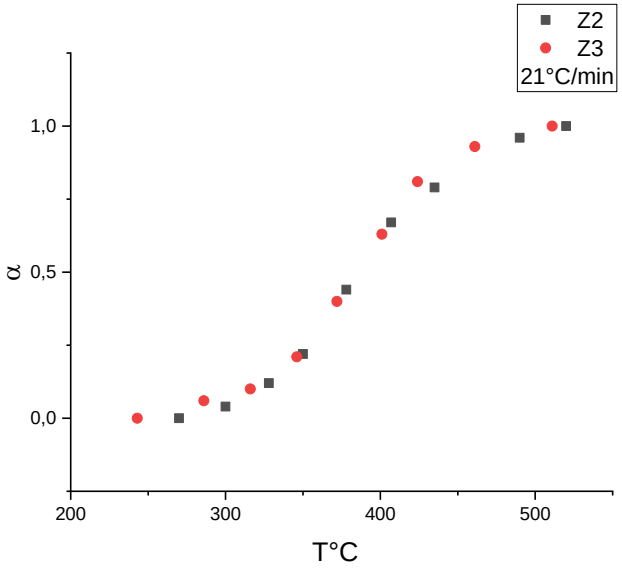

Fig 8:-Thermograms in α of the hydropyrolysis of the Z2 and Z3 layers at heating rates Θ=21°C/min.4

2.4: Coast-Redfer method:

In this work,as the last article**(A.Attaoui: 2023)**, a mathematical method is presented to arrive at kinetic constants and to choose the mechanism that best fits with the experimental results and that will take into account the physical and chemical reality of the system studied. This method is the Coats-Redfern method:

The rate equation for the decomposition reaction is expressed as:

$d\alpha/dt = ko\,(1-\alpha)^{n}\, e^{-E/RT}$(1) with $Koe^{-E/RT}$ the Arrhenius constant

or

$d\alpha/dT = ko\,(1-\alpha)^{n}\, e\text{-}E/RT\,/\theta$

The total variation of α as a function of temperature will be:

$F(\alpha) = d\alpha/(1-\alpha)\,n = ko\, e\text{-}E/RT\, dT/\theta$(2)

If x= E/RT, the integration of the second member of equation (2) gives the exponential integral function $p(x) = f^{\infty}_{x} e^{-x}/x^{2} dx$. This integral can be calculated for each value of x. However, to avoid the long calculations that this would cause, many authors have given approximate forms of this function. Coats-Redfern gave a form that is based on the asymptotic expansion of p(x) and is easier to use. This series expansion gives:

$f^{\infty} e^{-x}\, x^{-b}\, dx \sim x^{1-b}\, e^{-x} \sum (-1)^{n} (b)^{n}/x^{n+1}$ (3)

The latter leads to expression (4) by integrating the first member of equation (2).

$1-(1-\alpha)^{1-n}/1-n = k_{o} RT^{2} (1-2RT/E) \exp(-E/RT)/\theta E$ pour $n \neq 1$ (4)

$-Ln(1-\alpha) = koRT^{2}(1-2RT/E)\exp(-E/RT)/\theta\, E$ pour n=1

It is therefore possible to determine the value of the apparent activation energy from the slope of the line by plotting:

$Ln[-Ln(1-\alpha)/T^{2}] = f(1/T)$ pour n = 1

or (5)

$Ln[1-(1-\alpha)^{1-n}/T^{2}(1-n)] = f(1/T) = f(1/T)$ pour $n \neq 1$

To arrive at the activation energies we use order 1 **(A.Attaoui: 2023)** and adopt the first equation:

$Ln[-Ln(1-\alpha)/T^{2}] = f(1/T)$ pour n = 1

2.5: Activation energies for the decomposition of organic matter under hydrogen in non-isothermal (Θ=21°C/min)

The calculations to be made using the Coast-Redfern equation for n=1 and for a heating rate of 21°C/min and of Z2 and Z3 layers can be found in the following tables:

Table 2:- Calculs by Coast- Redfern for Z2 layer.

(1-α)	1/T	$1/T^2$	$\frac{-\ln(1-\alpha)}{T^2}$	$\frac{-\ln(-\ln(1-\alpha))}{T^2}$
0,88	$1,66\ 10^{-3}$	$2,76\ 10^{-6}$	$0,353\ 10^{-6}$	14,9
0,78	$1,61\ 10^{-3}$	$2,59\ 10^{-6}$	$0,644\ 10^{-6}$	14,3
0,56	$1,54\ 10^{-3}$	$2,37\ 10^{-6}$	$1,37410^{-6}$	13,5
0,33	$1,47\ 10^{-3}$	$2,16\ 10^{-6}$	$2,395\ 10^{-6}$	12,9
0,21	$1,41\ 10^{-3}$	$1,99\ 10^{-6}$	$3,10610^{-6}$	12,7
0,04	$1,31\ 10^{-3}$	$1,71\ 10^{-3}$	$5,504\ 10^{-6}$	12,1

Table 3:- Calculs by Coast- Redfern for Z3 layer.

(1-α)	1/T	$1/T^2$	$\frac{-\ln(1-\alpha)}{T^2}$	$\frac{-\ln(-\ln(1-\alpha))}{T^2}$
0,9	$1,710^{-3}$	$2,89\ 10^{-6}$	$0,30410^{-6}$	15,0
0,79	$1,6210^{-3}$	$2,62\ 10^{-6}$	$0,618\ 10^{-6,}$	14,3
0,6	$1,55\ 10^{-3}$	$2,40\ 10^{-6}$	$1,226\ 10^{-6}$	13,6

0,37	1,48 10^{-3}	2,19 10^{-6}	2,17710^{-6}	13,0
0,19	1,43 10^{-3}	2,04 10^{-6}	3,38810^{-6}	12,6
0,07	1,36 10^{-3}	1,85 10^{-6}	4,910 10^{-6}	12,2

We show the figures y= -ln(- ln(1-α)) = f(1/T) for the two layers
T^2

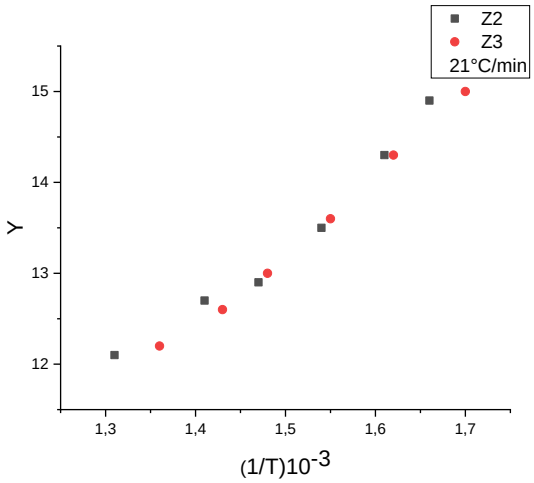

Fig 8:- Linearization according to Coast-Redfern for an order n=1 of the two layers Z2 and Z3forhydropyrolysis of kerogen

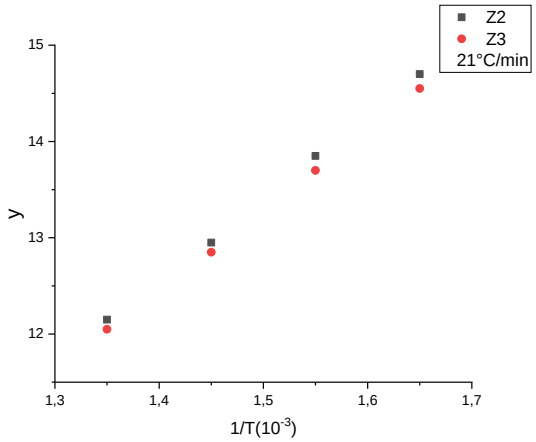

Fig 9:- Linearization according to Coast-Redfern after simulation for an order n=1 of the two layers Z2 and Z3for hydropyrolysis of kerogen.

Taking the equation y= -ln(- ln(1-α)) = f(1/T) according to Coast-Redfern approximations for
T^2
n =1. The slope is equal to E/R and the intersection with the ordinate axis is: -ln (koR (1-2RT/E)) assuming again that this value is a constant according to Coast-Redfern despite containing temperature as a value. We end up with activation energies as follows:

Samples	Ea (kj/mole)
Z2	71,06
Z3	69,64

2.6: Modeling for the extension of the activation energies of the other layers at different heating rates.
Activation energy is an extensive quantity and the Coast-Redfern equation can be applied using several approximations. For order n=1 we have:

$-Ln (1- \alpha) = koRT^2 (1-2RT/E) \exp(-E/RT) / \Theta E$ for n=1
We go to -Ln and this becomes:
$-Ln (-Ln ((1-\alpha) / T^2)) = -Ln (koR (1-2RT/E) / \Theta E + E/RT$ so it is a straight line of the form
$y = px + k$
$y= -Ln (-Ln ((1-\alpha) / T^2))$
$p= E/R$
$x= 1/T$ and
$k=-Ln (koR (1-2RT/E) / \Theta E)$

Coast-Redfern considers that the term $k=-Ln (koR (1-2RT/E) / \Theta E)$ is a constant even though it depends on T.

As energy is an extensive quantity, and as the second term of the Coast-Redfern equation is a constant, we will look for the quantity of energy at maximum velocity, i.e. at the temperature of the DTG peak, which we will call $E_{1/2}$ since α at this temperature (DTG) is equal to 1/2, so :
$E_{1/2} =RT(DTG)(-Ln (-Ln ((1-0.5) / T^2 (DTG)) - k)$
At the DTG peak, the constant k is assumed to be negligible:

$E_{1/2} =RT(DTG) (-Ln ((1-0.5) / T^2 (DTG))$.
We'll do the calculation for the Z2 layer (21°C/min).
According to Table 1: T (DTG) = 404°C= 677°K
$E_{1/2} = (0.3665 + 13.04) \times 4.18 \times 2 \times 677 =75.88$ kj/mol
Now, when we look for the activation energy of the Z2 layer (Θ=21°C/min) using the slope, we find (previous paragraph)
$E_{total} =71.06$ kj/mol which is an energy lower than $E_{1/2}$
So in this case for organic matter we will assume that
$E_{total}= E_{1/2} - E_S$
E_S is the energy that must be subtracted and is due to the model adopted.
$E_S=75.88 - 71.06 = 4.82$ kj/mol
This energy E_S will be subtracted when we are in a cold climate.
The same reasoning will be used for tick Z3 (21°C/min).
According to Table 1: T(DTG) = 401°C= 674°K
$E_{1/2} = (0.3665 + 13.02) \times 4.18 \times 2 \times 674 =75.43$ kj/mol
Now, when we look for the activation energy of the Z3 layer (Θ=21°C/min) using the slope, we find (previous paragraph)
$E_{total} =69.64$ kj/mol which is an energy lower than $E_{1/2}$
So in this case, in the same way as for organic matter, we will assume that
$E_{total} = E_{1/2} - E_S$
E_S is the energy that must be subtracted and is due to the model adopted.
$E_S=755.43 - 69.64 = 5.79$ kj/mol
This E_S energy will be subtracted when we are in a warm climate.
We will subtract this energy depending on whether we have a cold climate (Z0 and Z2)
$E_S = 4.82$ kj/mol
Similarly, we will use this energy when we are in a warm climate (Z1, Z3 and Z4)
$E_S = 5.79$ kj/mol
For a cold climate (Z0 and Z2)
$E_{Total} = (E_{1/2} - 4.82)$kj/mol
For a warm climate (Z1, Z3 and Z4)
$E_{Total}= (E_{1/2} - 5.79)$ kj/mol
In the following table, we have calculated the total activation energies for the layers at different heating rates (except for the Z0 layer where the thermobalance did not indicate the temperature T (DTG)), by applying the form
$E_{1/2} = (-Ln-Ln (0.5) + Ln T^2 (DTG))$. RT (DTG), given the temperature values in Table 1.

Table 4:- Activation energy of organic matter hydropyrolysis for different layers at different heating rate.

Heating rate (°C/min)	**Characteristics**	**Samples**
	Origin	Tarfaya

	Zone	Z_0	Z_1	Z_2	Z_3	Z_4
21	DTG peaktemperature °C	-	427	404	401	398
	Activation energy (kj/mole)	-	73,02	71,06	69,64	69,30
15	DTG peak temperature °C	-	411	386	390	377
	Activation energy (kj/mole)	-	69,94	68,71	68,24	66,57
09	DTG peak temperature °C	-	392	373	379	368
	Activation energy (kj/mole)	-	68,52	67,04	66,85	65,46

From the thermograms in the previous paragraph, we can see that the curves overlap to a certain extent, meaning that the reactivity is the same for all the layers. This can be discerned by observing the temperatures of the DTG peaks, which are slightly different. Looking at the activation energies, we can see that the energy balance decreases with depth, and this holds true for all three heating rates.

Figure 10 below shows these activation energies as a function of the layers in the deposit. Note that the Z0 layer didn't show up because there are no DTG peaks in this layer.

This figure shows the histograms of activation energies for this hydropyrolysis reaction for the different layers at different heating rates.

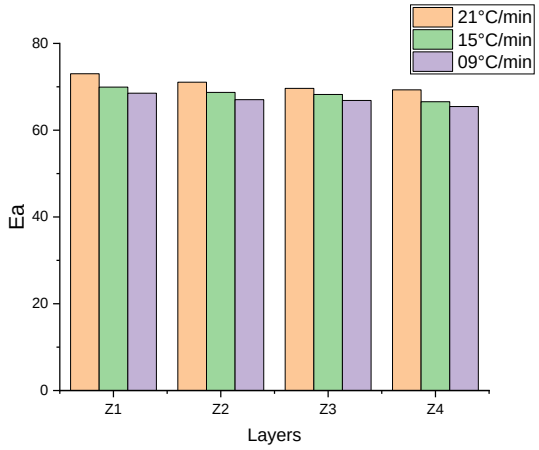

Fig 10:- Histograms of activation energies for the different hydropyroplysis layers.

Figure 11 also shows the variation in this energy for the different layers at different hydropyrolysis heating rates.

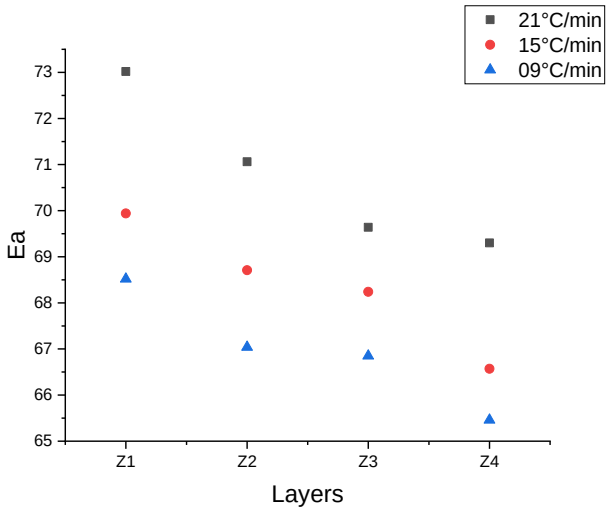

Fig 11:- Variation in activation energy as a function of oil shale layers.

We note that this energy varies in the direction of a decrease according to the depth, i.e. the reactivity increases with this depth, unlike carbonates (mineral matrix) where we have noted that the reactivity depends on the climate of the geological stage of formation **(A.Attaoui: 2023).**

Conclusion:-

Access to the activation energies for the dynamic regime in true thermogravimetry depends on the development model used, and we have cited several development models which generally derive from Arrhenius' law. The values found are relative to the method chosen and the experimental technique **(J.M. Charlesworth: 1985).**

In this work, using the Red-Croft as a thermobalance (a Setaram), we carried out the hydropyrolysis of organic matter (kerogen) as the objective for analyzing the different layers of the Tarfaya deposit. Looking at the thermograms, the location of the curves □ =f(T) in relation to each other indicates that the samples have similar reactivity, whereas for the DTG, a difference in the maximum temperature of the peaks is to be noted, which we will try to discern later. This shows the reactive effect of hydrogen on the same type of organic matter, where the decisive stage is the same.

Shale samples with different reactivities under an inert gas will have the same reactivity in the presence of hydrogen. In addition, the organic matter concentration threshold, above which hydropylosis is the same for all samples, is 6.86% apart from Z0. The low reactivity of Z0 compared to the other zones can be explained by its low organic matter concentration. It has been shown that during thermal degradation, pyrolytic oil acts as a catalyst in this reaction.

Coasr-Redfern as a development model for arriving at activation energies was usedinthermogravimetry under dynamic conditions, the approach equation for order one being :
$-Ln (1- \alpha) = koRT^2 (1-2RT/E) \exp(-E/RT) / \Theta E$ for n=1
When we go to -Ln this becomes:
$-Ln (-Ln ((1-\alpha) / T^2)) = -Ln (koR (1-2RT/E) / \Theta E) + E/RT$ so it's a straight line.

The activation energies found by the method (21°C/min) are: 71.06 kj/mol for the Z2 layer
and 69.64 kj/mol for the Z3 layer.
Since energy is an extensive quantity, and since the second term of the Coast-Redfern equation is a constant, we will look for the quantity of energy at the maximum velocity, i.e. at the temperature of the DTG peak, which we will call $E_{1/2}$ since α at this temperature (DTG) is equal to 1/2, i.e, so :
$E_{1/2} = RT(DTG)(-Ln (-Ln ((1-0.5) / T^2 (DTG)) - k)$
At the DTG peak, the constant k is assumed to be negligible. When looking for

the energy $E_{1/2}$, we have 75.88 kj/mol for Z2 and 75.43 kj/mol for Z3, so it is logical to consider that there is a surplus of energy by the methodology, so for the organic matter we assume
Total $E = E_{1/2} - E_S$
E_S is the energy that must be subtracted and is due to the model adopted.
E_S=75.88 - 71.06 = 4.82 kj/mol for Z2, and E_S=755.43 - 69.64 = 5.79 kj/mol for Z3. Finally, we arrive at the model:
For a cold climate (Z0 and Z2) Total $E = (E_{1/2} - 4.82)$kj/mol
For a warm climate (Z1, Z3 and Z4) Total $E = (E_{1/2} - 5.79)$ kj/mol.
The results deduced from the approximation model can be found in the following table:

Heating rate (°C/min)	**Characteristics**	**Samples**				
	Origin	Tarfaya				
	Zone	Z_0	Z_1	Z_2	Z_3	Z_4
21	Activation energy (kj/mole)	-	73,02	71,06	69,64	69,30
15	Activation energy (kj/mole)	-	69,94	68,71	68,24	66,57
09	Activation energy (kj/mole)	-	68,52	67,04	66,85	65,46

From the thermograms in the previous paragraph, we can see that there is a certain superimposition of curves which may indicate that the reactivity is the same for all the layers, but this can be discerned by observing the temperatures of the DTG peaks, which are slightly different. If we look at the activation energies, we see that the energy balance decreases with depth, and this holds true for all three heating rates, whereas for carbonates (mineral matrix), where we have noted that reactivity depends on the climate at the geological stage of formation (A.Attaoui: 2023).

Reference:-

[1]A.Attaoui, Modeling and non-linear mechanisms in heterogeneous kinetics of the no isothermal pyrolysis orhydropyrolysis for Tarfaya oil shale (Morocco), Int.J.Adv.Res,DOI:10.21474/IJAR01/16486,Mars 2023, 11(03), 712-723
[2] M. Enomoto and all.Journal of japan Petroleum Instit.Vol 28 N°2 1985.
[3] M. Enomoto and all. Journal of Japan Petroleum InstitVol 25 N°5 1982.
[4] E. Fuzimsky and all. Fuel.Proces.Techno. 8. 1984. 293.
[5] P.A. Lunch and J.C. Janta et al American. Chem. Soci. Symp.St Louis 1984 April 2-13.
[6] S.D. Carter and all Fuel. Vol. 69. 1990. Sept. 1124.
[7] J.C. Janka, R.C. Rex. AICHE.1984 August.19-22.
[8] J.C. Janka and J.M. Dennison, Paper presented at 10T Sympoon synthetic. Fuel.From oil shale, Atlanta, Georgia. Dec. 3-6. 1979.
[9] R.D. Matews and all.AAPG. Bulletin Vol. 65. N° 5. 1981. 53.
[10] Vyazovkin S, Burnham AK, Criao JM, Pe'rez-Maqueda LA, PopescuC,Sbirrazzuoli N. ICTAC kinetics committee recommendations for performing kinetic computations on thermal analysis data. ThermochimActa 2011
[11] A.W.Coats and d.P.Redfern. Nature (London), 201.1964.68.
[12] Z.S.Freeman and B.Carroll.J.Phys.Chem. 62.1952.394. D.B D.
[13]Anthony and J.B.Howard. AICHE.D22.1976.625.[5]H.L.Friedman.J.Polym.Sci.C6.1965.183.
[14] S.M.Shin and H.Y.Sohn. Ind. Eng. Chem. Proc. Des.Dev.19.1980.420.
[15] M.Suzikietal.Chem.Eng.Jpn.13(3)1980.249.
[16] Lee and Beck.AICHE.Vol.30.N°31984.May.517-519.
[17]V.M.Gorbachev.J.Thermal.Anal.10.1976.477.
[18] R.K.Agrawal,M.S.SivasubramanionAICHE.Vol33N°71987.July1212.
[19] S.V.Vyazovkin et al. Journal of thermal Analysis Vol 32 .1987
[20] I.E.Cuthrell et al AICHE.Vol33N°81987.August.
[21] Z.Smieszekiandall.Journalofthermal.AnalysisVol32.1988.377
[22] Ahmed Malal, Doha Lahmadiand A .Attaoui, "Type of burial and adaptation of the geological ages with the sedimentation of the organic matter for the different layers for the Tarfaya's oil shale deposit (Morocco) ,Int.J. Adv. Res.DOI:10.21474/IJAR01/14557, April 2022,10(04),372-382.

[23] K.M. Jeong and J.F. Patzer ACS Symp. Series N° 230. Amer. Chem. Soc. Washington D.C. 1983. P.529.
[24]A.AttaouiActivation energies by Coast-Redfern approximations of the mineral matter hydropyrolysis for the Tarfayaoilshale(Morocco).Modelingtoobtainthese energiesforthe differentlayersinnon-isothermal.Int.J. Adv. Res DOI**:**10.21474/IJAR01/17280, July 2023, 10(07),712-724
[25] J.M. Charlesworth. Ind. Eng. Process Des.Dev.Vol. 24 N°4 1985.